

Particularities of structural transformations in welded joints of deformable aluminium alloys, hardenable by aging

for obtaining the scientific title of doctor at Polytechnic University of Timișoara

in the PhD field Materials Engineering

author ing. Ciprian Pavel LUCIAN

scientific coordinator Prof.univ.dr.ing. Ion MITELEA

Cap. 1 Current state of research in obtaining of welded joints from aluminium alloys

1.2. Microstructure and properties of aluminum alloys

The main alloying elements that are part of Al-based commercial alloys are: magnesium (Mg), silicon (Si), manganese (Mn), zinc (Zn) and copper (Cu). According to international specifications [32], alloys are distinguished by four-digit numbers, the first digit characterizing the group or series to which the alloy belongs: 1xxx (Al99,99 ... Al99,5),

- 2xxx (AlCu),
- 3xxx (AlMn),
- 4xxx (AlSi),
- 5xxx (AlMg (Mn)),
- 6xxx (AlMgSi)
- 7xxx (AlZnMg (Cu)),
- 8xxx(others, for example, AlFe, AlLi).

All aluminum alloys can be classified into the following three main groups:

- deformable alloys, intended for the manufacture of semi-finished products and finished parts by rolling, pressing, forging, stamping, etc. In turn, they are divided into alloys hardenable by heat treatment and non-hardenable by heat treatment;
- alloys casted into parts;
- alloys obtained by powder metallurgy.

The main difference between non-hardening alloys and those hardenable by heat treatment lies in the hardening mechanisms by cold deformation, respectively by hardening for solution

followed by natural or artificial aging which are responsible for increasing the characteristics of mechanical strength.

1.3. Mechanisms for consolidating deformable, non-hardenable alloys through heat treatment

This group of materials includes pure aluminum and the types of alloys Al-Mg, Al-Mn, Al-Mg-Mn and Al-Fe. The hardening mechanisms act on them by cold deformation and by the formation of solid solutions.

Hardening by solid solutions involves the incorporation of the atoms of the alloying elements in the crystal network of aluminum. Up to a certain content of foreign atoms, this effect can be significant. The incorporation of alloying atoms prevents the sliding processes in the crystal network, resulting in an increase in the values of mechanical strength.

In order to restore the mechanical properties, the annealing heat treatment for recrystallization is usually applied. The heating temperature is above approx. 350 °C. The maintenance time should not be too long as it causes an increase in grain size. For alloys of class 5000 (Al-Mg and Al-Mg-Mn) with more than 3% Mg, special cooling conditions are considered in order not to damage the intercrystalline corrosion behavior.

1.4. Mechanisms for consolidating deformable, hardenable alloys through heat treatment

Hardening arises by usually combining two or three alloying elements with aluminum. This includes alloys from the 2xxx, 6xxx and 7xxx series (Al-Cu-Mg, Al-Mg-Si and Al-Zn-Mg (Cu). Heat treatment of solution quenching must take into account the following premises:

- A continuous variation of the solubility of the alloying element in the crystalline network of aluminum, with the decrease of the temperature in solid state;
- Formation of finely dispersed precipitates in the metal network.

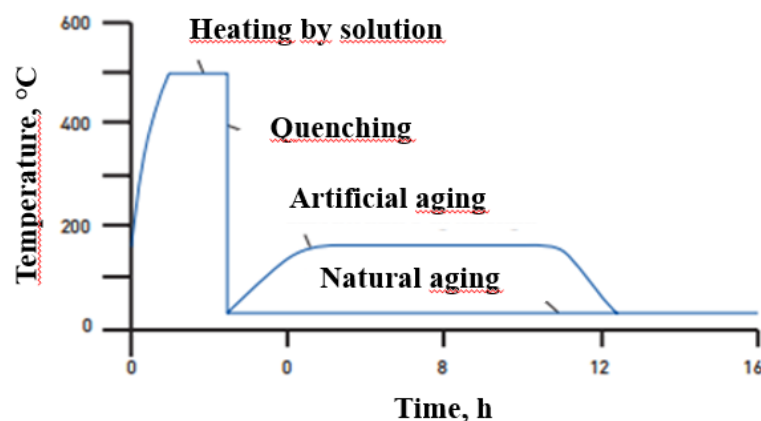


Fig.1.5 Heat treatment for solution cyclogram followed by aging [30]

1.5. Structural changes in fusion welding. Elements of difficulty

Although the melting temperature of aluminum is relatively low, the heat required for aluminum fusion welding is about the same size as for welding steel. The reason for this is the high thermal conductivity of the material. The effect of the welding heat is manifested by the appearance of unwanted structural changes and by deformations of the welded components.

One of the difficulties in using welded structures in these alloys is the general reduction in the mechanical properties of the welded joint areas compared to the base material. This is due to the lower mechanical strength of the welded seam and the deterioration of the initial structure of the ZIT under the action of thermal welding cycles.

Also, the effects of welding heat on the phenomena of precipitation and cracking by liquefaction, which are responsible for the worsening of the mechanical properties of welded joints are incompletely analyzed [41].

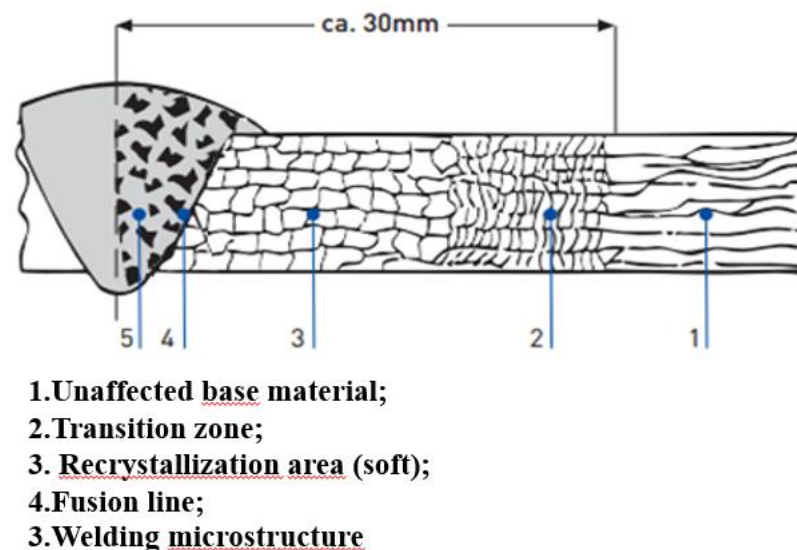


Fig.1.7 Zonele microstructurale ale unei îmbinări sudate prin topire [83]

1.6. Heat treatments before, concomitant and after welding

For larger cross sections of material, it may be necessary to preheat the components to be welded. Preheating temperatures should not exceed the limit of 200 ° C. This treatment in conjunction with the welding operation applies to all categories of aluminum-based alloys. Residual stresses inevitably arise in a welded construction. Their level is significantly influenced by the construction geometry, the welding process and the welding sequence.

The post-welding application of the annealing heat treatment for detensioning will be done to a very limited extent. In addition, the entire welded assembly must be placed in the furnace and the treatment parameters must not change the structural state of the material. Usually, the annealing temperature has values in the range of 250 – 350 ° C .

In general, it should take in consideration that strain relief annealing can cause greater deformation of the components. Welded metal constructions from EN AW-7020 T6 (DIN 1725: AlZn4.5Mn F35 / F34), can only be put into operation after the completion of the natural aging process.

1.7. Incompatibility problems for obtaining heterogeneous welded joints

1.7.1. Generalities

Joining of dissimilar materials by techniques that ensure a metallic continuity is based on the fruiting of a favorable combination of properties such as::

- good mechanical properties of one material and a low specific mass of the other material;
- good mechanical properties of one material and good corrosion stability of the second material;
- good mechanical properties of one material and good electrical properties of the other material.

1.8. Welded joints of dissimilar materials, Al alloys - steels

The difficulties that occur in welding dissimilar materials are due to differences in thermal, mechanical and structural properties. However, there is a growing trend in the use of heterogeneous joints in giant industries that include shipbuilding, military vehicles, the aerospace industry and the automotive industry. The use of metallic materials with low specific mass instead of the heaviest ones allows to reduce the fuel consumption and even the production costs.

A number of research papers have aimed to find welding processes of these dissimilar alloys, but the problem of loss of mechanical strength characteristics of the welded area due to the formation of brittle intermetallic phases has not been solved [47] [2] [11] [78] [67]. Due to differences in thermal properties, coefficients of expansion, thermal capacity and conductivity, crystal lattice, melting temperatures (660 ° C for aluminum and 1500 ° C for steel) and near-zero solubility in the solid state of iron in aluminum, which causes deformations and porosities and cracks appear which lead to the reduction of the mechanical properties of the welded joints.

1.9. MIG and WIG welded joints

WIG welding of an aluminum alloy (5A06 AlMg) with an austenitic stainless steel was performed using an aluminum-based filler and a non-corrosive flux (fig.1.10). The results indicated the formation of fragile intermetallic phases with a thickness of 5 - 35 μm [36] such

as: $\tau_5\text{-Al}_{7.2}\text{Fe}_2\text{Si}$, $\eta\text{-Fe}_2\text{Al}_5$ and FeSi_2 . The breaking strength was 140 MPa. The rupture occurred in the metal deposited at the corner of the joint area. The formation of these phases can be predicted by ternary phase diagrams (fig. 1.11) and if the correct path has been chosen, the nucleation of these types of phases can be prevented.

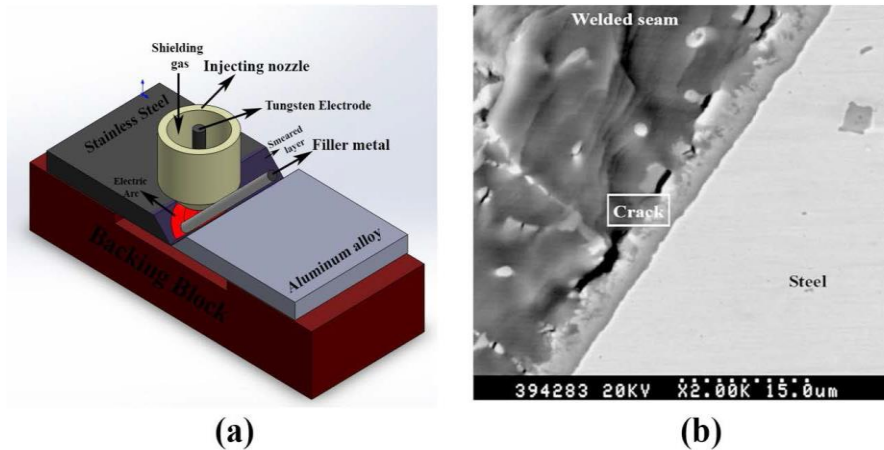


Fig.1.10 a) WIG welding of Al-stainless steel alloy; b) cracks on the interface [36] [67]

1.10. Laser and electron beam welded joints

A low carbon steel was welded with an aluminum alloy (5754) in keyhole welding mode with overlapping configuration, using laser technique [48].

To reduce the formation of intermetallic phases during the welding process, the effect of laser power, pulse duration and overlapping factor was studied. With the increase of these three parameters the amount of intermetallic compounds in the welded area was increased, while the decrease of these main parameters led to the appearance of cracks in the weld (fig.1.13).

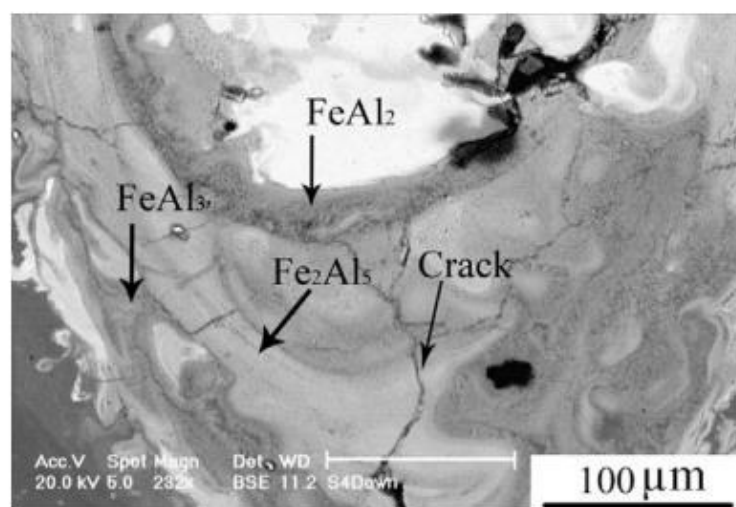


Fig.1.13 Imaginea SEM a sudurii cu fisuri si compusi intermetalici [48]

1.11. The objectives of the doctoral thesis

The combination of materials of the same or different nature remains a topical issue as it cannot always be done with the help of common techniques such as: manual arc welding, MIG welding, WIG welding, etc. Application of MIG / MAG welding in pulsed current or laser brazing can lead to incompatibility problems between aluminum alloys of the same nature or between them and steels.

Therefore, in the research carried out, a first objective is to achieve homogeneous welded joints that by heat treatment after welding to have characteristics of mechanical strength as close as possible to those of the base metal.

The second important objective is to study the process of laser brazing of deformable alloys from the 6xxx series (AlMgSi) with low galvanized alloy steels.

By changing the chemical composition of the welding bath, an attempt is made to limit the formation of fragile intermetallic phases between iron and aluminum, and the working environment of the welding process will avoid the rapid oxidation of aluminum.

A final objective proposed in the paper is the friction welding with rotating active element of deformable aluminum alloys with austenitic stainless steels.

Cap.2 Research on the MIG welding process in pulsed current of deformable alloys, hardenable by aging

2.2. Material examined and working procedure

The aluminum alloy used in the experiments, brand 6082 - T6, (AlSi1MgMn according to EN 573) was delivered in the form of sheets with a thickness of 5 mm, heat treated by hardening for solution, $535 \pm 5 \text{ }^\circ\text{C} / 25 \text{ min.} / \text{water}$, followed by artificial aging, $175 \pm 10 \text{ }^\circ\text{C} / 8 \text{ h} / \text{air}$.

The nominal chemical composition of the alloy sheets used to make penetrated butt joints is: Si = 1.18%, Fe = 0.39%, Cu = 0.065%, Mn = 0.70%, Mg = 1.32%, Cr = 0.10%, Ni = 0.015%, Zn = 0.044%, Ti = 0.011%, Ga = 0.01%, V = 0.023%, Al = Rest.

The AlSi 5 electrode wire (Alloy 4043) was selected as the filler material according to ISO 18273 and EN 573-3 with a diameter of 1.2 mm, which has the following chemical composition requirements: Si = 4.5 - 6.0%, Fe \leq 0.8% , Cu \leq 0.30%, Mn \leq 0.05%, Mg \leq 0.05%, Zn \leq 0.10%, Ti \leq 0.20%, Be \leq 0.0003%, Al = Rest.

The shielding gas was Argon 4.8 (purity \geq 99.998%), Linde, with a flow rate $Q = 14 - 15 \text{ l} / \text{min}$. The welding was done in horizontal position, position PA / SR EN ISO 6943, the

welding direction being to the left, and the inclination of the electrode wire, 85° . The preparation of the joint and the positioning of the components is presented in figure 2.1.

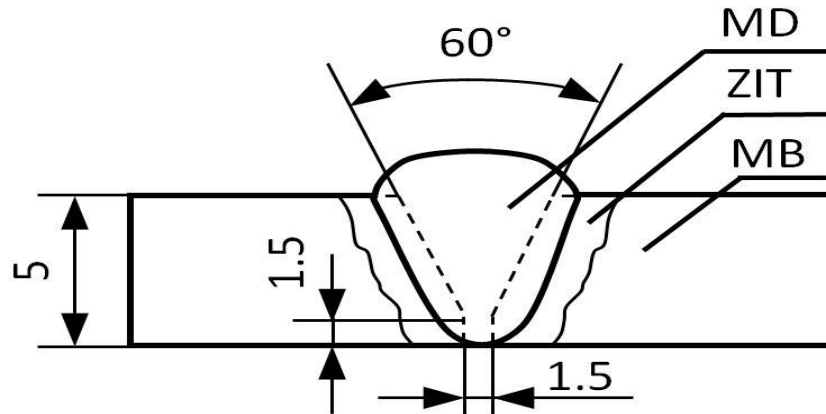


Fig.2.1 Geometry of the butt welded joint

The welded joints were made in one pass with the following welding technological parameters:

- Wire feed speed: 6.2 m/min.
- Welding medium current: ≈ 130 A
- Arc voltage: 23 V ($\Delta U_a = 0$)
- Pulse current: 220 A
- Pulse time: 2 ms
- Background current: 64 A
- Pulse frequency: 210 Hz
- Slope time: 9
- Self-regulating coefficients : $k_a = 36\%$; $k_i = 0\%$
- Welding speed : 25 cm/min



Fig.2.2 Welding experimental stand

2.3. Macrography of welded joints

For the examination of the overall structure and highlight the heterogeneities occurred in welded joints, samples with transverse faces (normal to the longitudinal welding axis), in accordance with standard techniques, were taken and prepared.

The appearance of the outer surface of the weld is shown in fig.2.7, and the macrographic image of a cross section through a welded joint is shown in fig. 2.8.

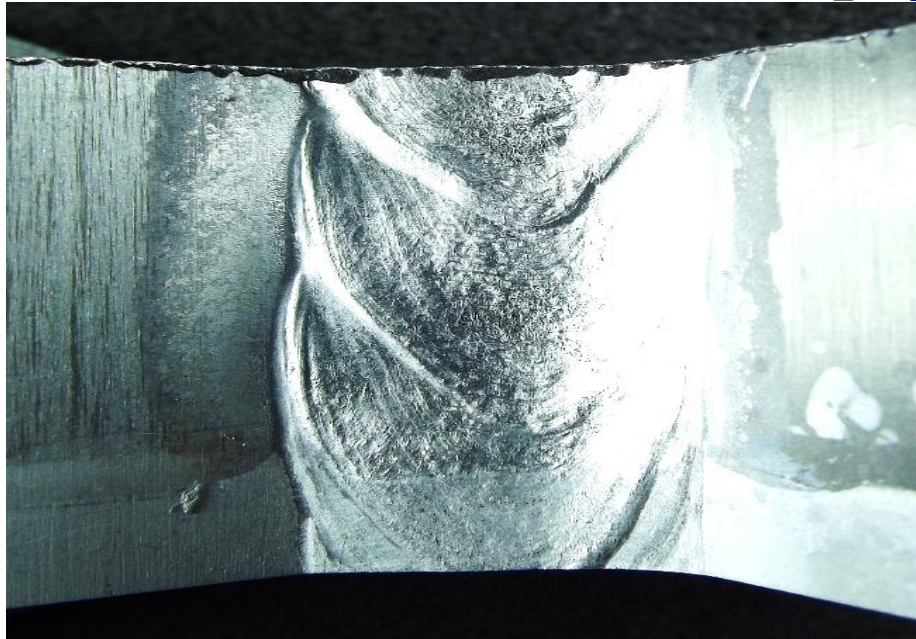


Fig.2.7 Macroscopic image of the outer surface of the weld seam

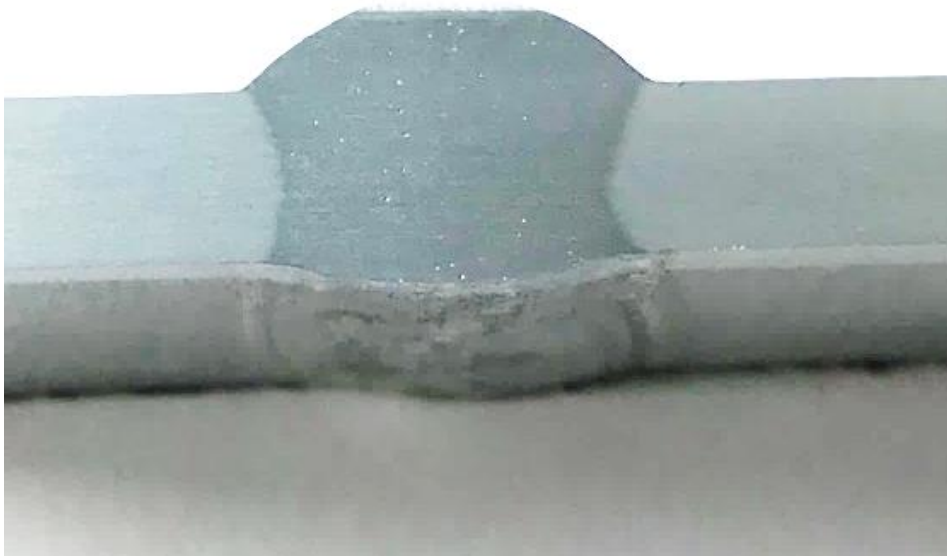


Fig.2.8 Macrograph of welded joint areas

2.4. Micrography of welded joints

Figures 8...10 show some microstructural images of the characteristic areas of the welded joints made with parameters established by the experimental tests. The chemical reagent used etching has the following chemical composition: 1 ml of 40%HF + 1.5 ml of concentrated HCl + 2.5 ml of concentrated HNO₃ + 95% of H₂O₂.

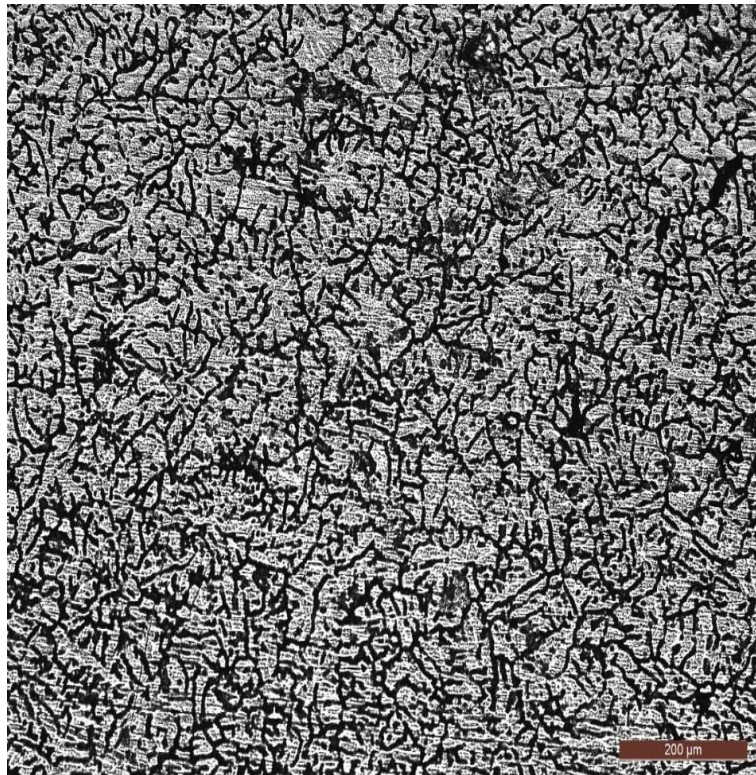


Fig.2.9 x 100 Microstructure of the welded bead

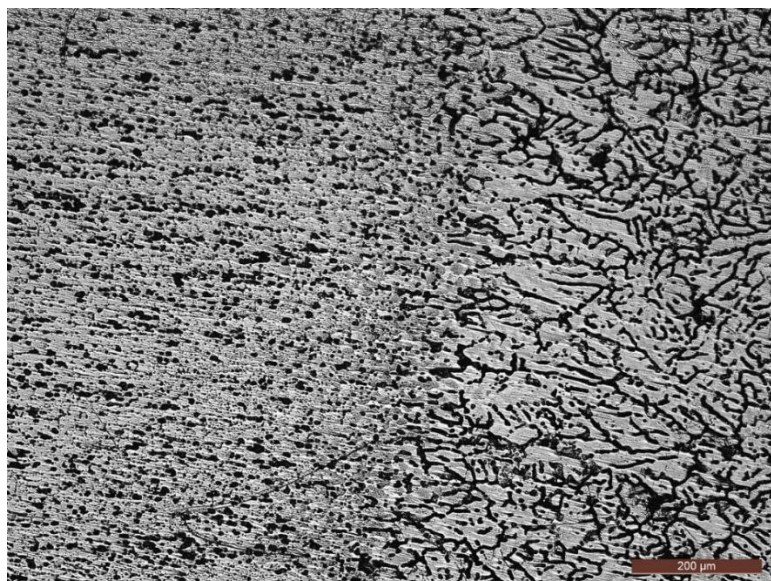


Fig.2.10 x100 Microstructure of the interface welding - base metal



Fig.2.11 x100 Base metal microstructure

2.5. Static traction tests

Tab.2.1 Values of static traction characteristics

No.	Source	Rm, N/mm ²	A5, %	Location of rupture
1	Base Material, BS	329	18,5	-
2	BS	327	14,5	-
3	BS	328	16,0	-
4	Welded Joint, WJ	200	9,6	HAZ
5	WJ	202	9,8	HAZ
6	WJ	201	9,8	HAZ
7	WJ	204	10,2	WELD
8	WJ	200	9,6	HAZ

2.6. Microhardness tests

As the hardness is the most sensitive mechanical characteristic to the structural changes occurred during the welding process, samples with transverse faces were taken from the joints made, which were subjected to such tests. Based on the obtained results, the graph from fig.2.12 was constructed.

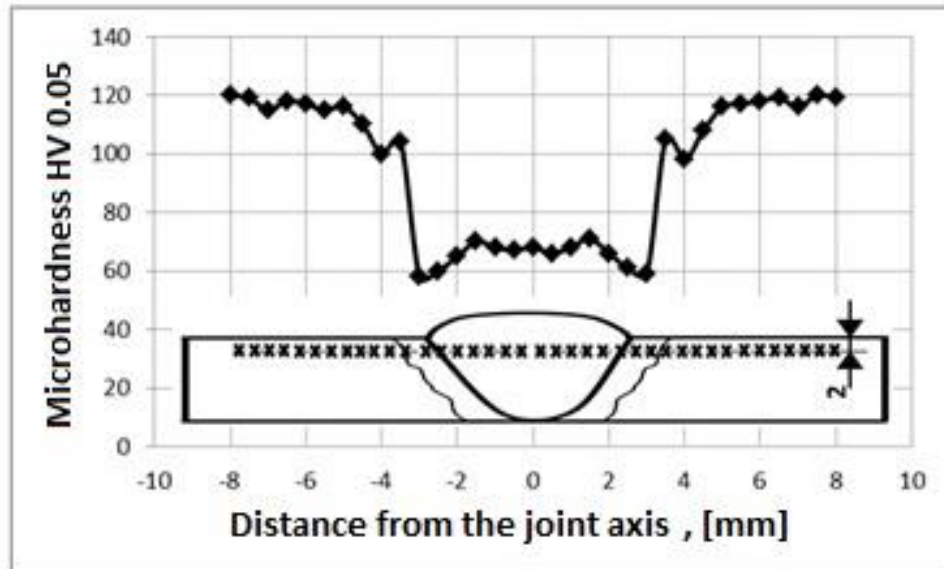
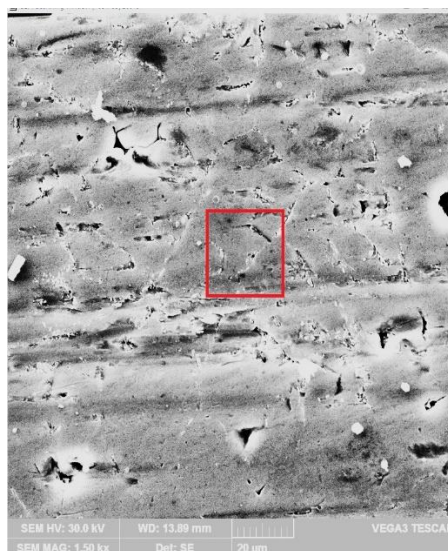


Fig.2.12 The hardness gradient curve on the cross section of the welded joint

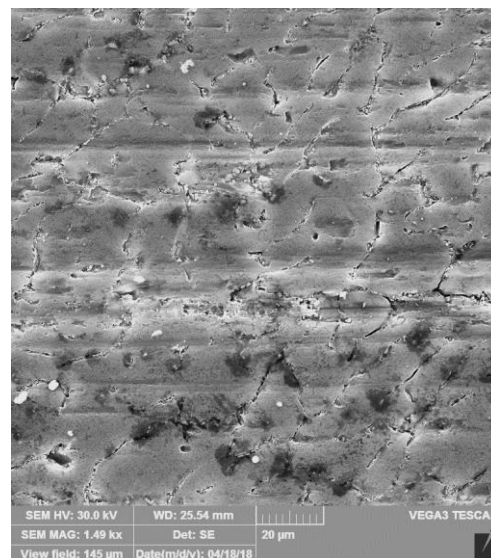
2.1. EDX investigations

X-ray energy dispersion analyzes aimed to determine the influence of the welding process on possible changes in chemical composition in the welded seam.

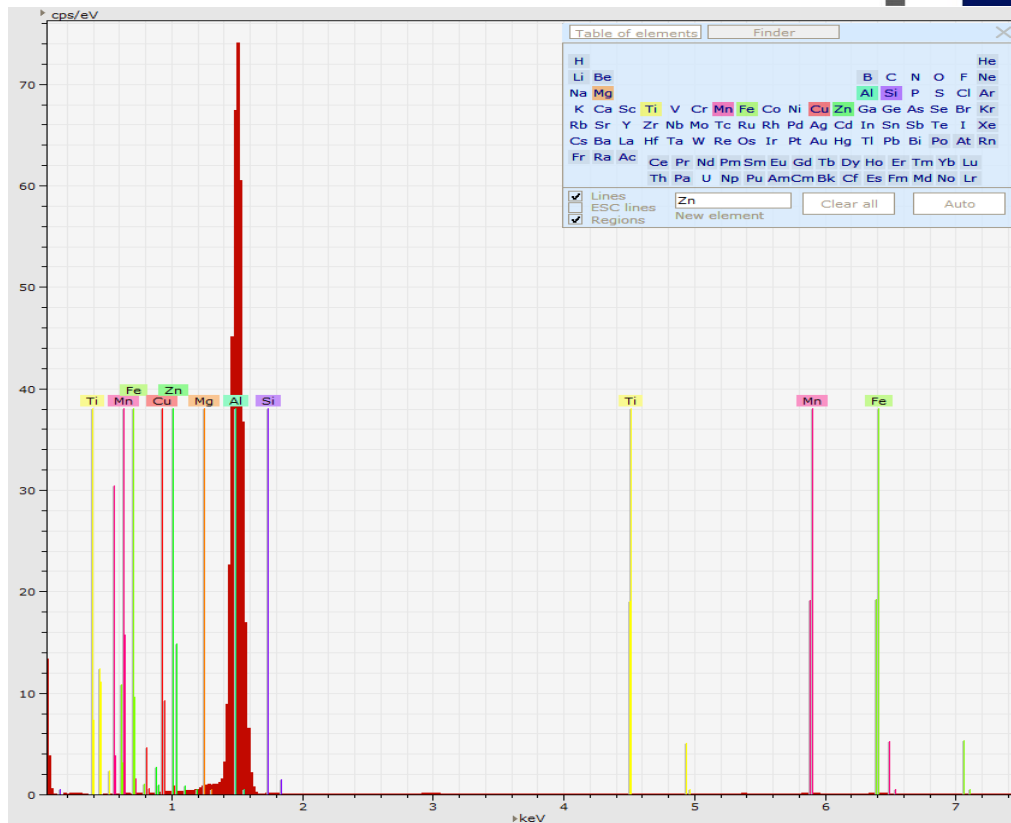
Figures 2.13 and 2.14 exemplify some microstructural images of welded seam and base metal, obtained by scanning electron microscope as well as X-ray energy dispersion spectra together with the local chemical composition of the two specific areas of the welded joint (welding + base metal).



(a)



(b)



(c)

	Series	unn. C [wt.%]	nor. C [wt.%]	Atom C [at.%]	Error (1 Sigma) [wt.%]
Titanium	K series	0.02	0.01	0.01	0.01
Magnesium	K series	1.88	1.22	1.35	0.14
Aluminium	K series	150.24	97.35	97.51	7.55
Silicon	K series	1.42	0.92	0.89	0.10
Manganese	K series	0.32	0.21	0.10	0.04
Iron	K series	0.41	0.27	0.13	0.04
Copper	K series	0.01	0.01	0.00	0.01
Zinc	K series	0.02	0.01	0.01	0.01
Total		154.33	100.00	100.00	

(d)

Fig. 2.13 SEM images (a), (b), dispersion spectrum (c) and local chemical composition (d) of welded seam

2.9. Conclusions

For the experimental conditions used, the breaking strength of the welded joints decreases by approx. 39% and the elongation at break with approx. 40% compared to the nominal values specific to the base metal. In the thermally influenced area, at a distance of approx. 2 mm from the joint axis there is a pronounced softening of the material (HV hardness decreases by about 45%), as a result of the aging phenomenon induced by the thermal welding cycle.

The mechanical properties of welded MIG aluminum alloy joints, EN AW 6082, can be restored by post weld heat treatment for solutioning followed by artificial aging.

Cap.3 Research on the laser braze-welding process of aluminum alloys with zinc coated low alloy steels

3.2 Research methodology. Experimental results

DX51D + Z100MA hot rolled and thermally galvanized steel is one of the basic materials used to perform brazing. The thickness of the zinc protection layer is 7 μm. The aluminum alloy sheet is from the 6082 - T6 series. The chemical compositions of these base materials are summarized in tab.3.2.

Tab. 3.2 Chemical composition of the two base materials

Material	C [%]	Si [%]	Mn [%]	P [%]	S [%]	Ti [%]	Fe [%]	Mg [%]	Cr [%]	Cu [%]	Al [%]
DX51D+ Z100MA	0,12	0,34	1,01	0,09	0,02 8	0,21	Rest	-	-	-	-
6082-T6	-	1,18	0,71	-	-	0,01	0,39	0,82	0,10	0,06	Rest

As filler material was selected AlSi12 wire according to DIN 1732 and ER4047 according to AWS A5.10, with a diameter of ϕ 1 mm. The chemical composition and melting temperature of this wire is presented in tab.3

Tab. 3.3 Chemical composition and melting temperature of the filler material

Material	Si [%]	Fe[%]	Cu[%]	Mn[%]	M[%]	Zn[%]	Ti[%]	Melting temperature, °C
AlSi 12	11-13	<0,60	<0,30	<0,15	<0,10	<0,20	<0,15	573 - 585

100% Argon was used as shielding gas with a flow rate of 10 l/min.

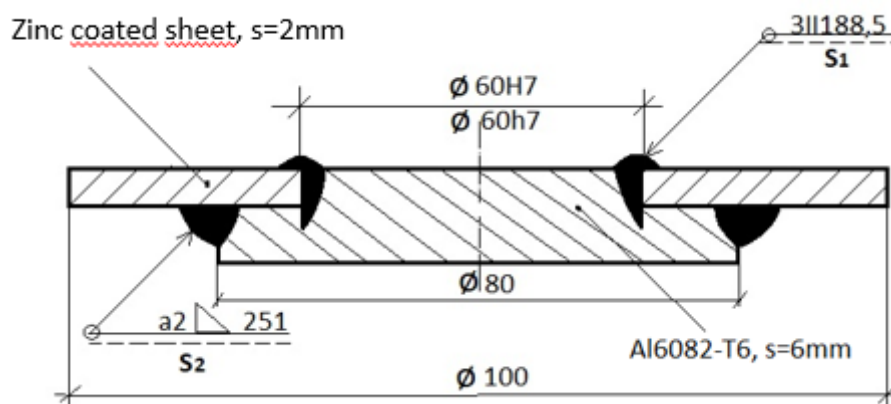


Fig. 3.6 Sample geometry for laser braze-welding



Fig. 3.8 Sample positioning and fixing device for braze-welding

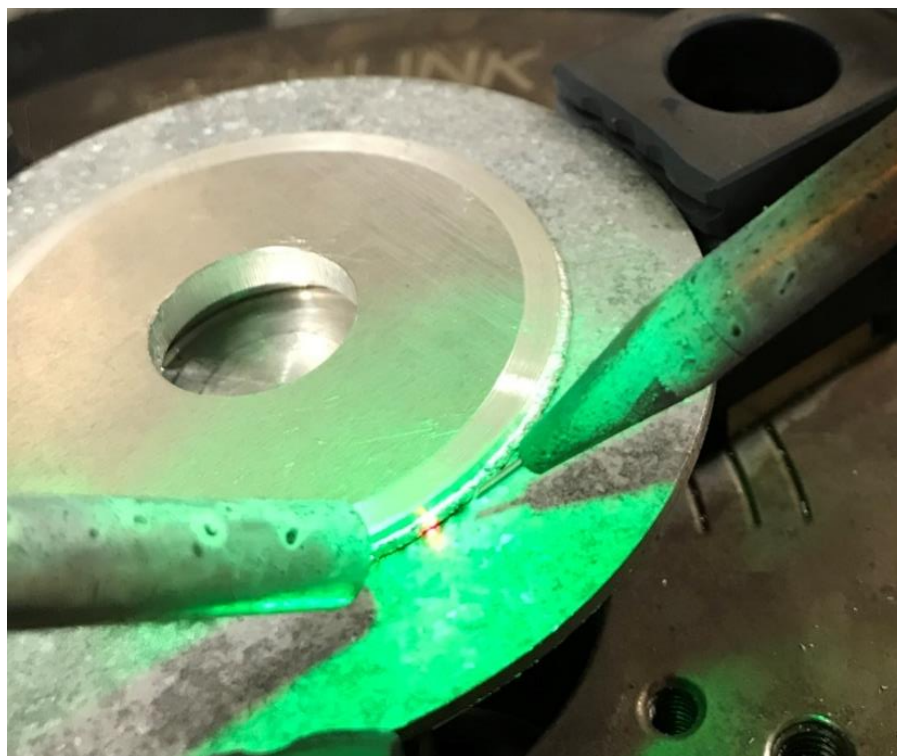
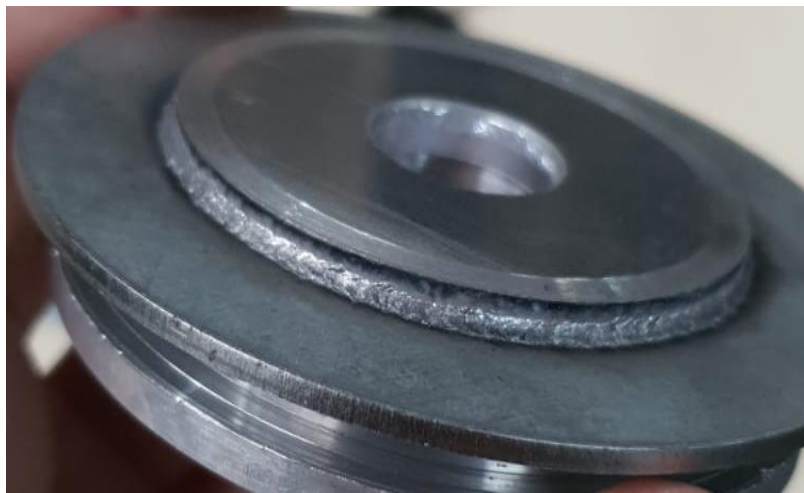


Fig.3.13 Exterior appearance of the weld

Tab.3.4 Braze-welding process parameters

Aluminium alloy / zinc coated steel	Power, [W]	Braze welding speed, [mm/min.]	Rotation angle of the part [degrees]	Advance speed AlSi12, [mm/min.]
Sample Set 1	1600	2600	363	2700
Sample Set 2	1700	2400	363	2900
Sample Set 3	1600	2600	363	2600
Sample Set 4 surface - verso	1700+1200	2400+3000	363	2900+1200
Sample Set 5 surface - verso	1600+1300	2600+3000	363	2600+3000



(c)

Fig.3.14 The appearance of the weld-brazed joint

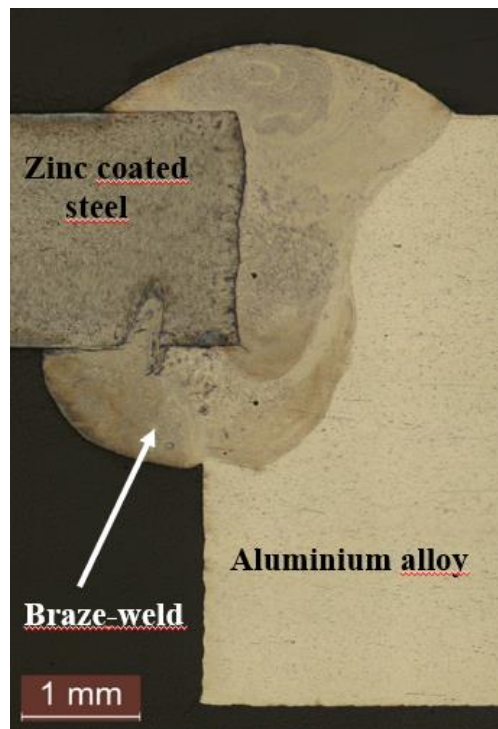
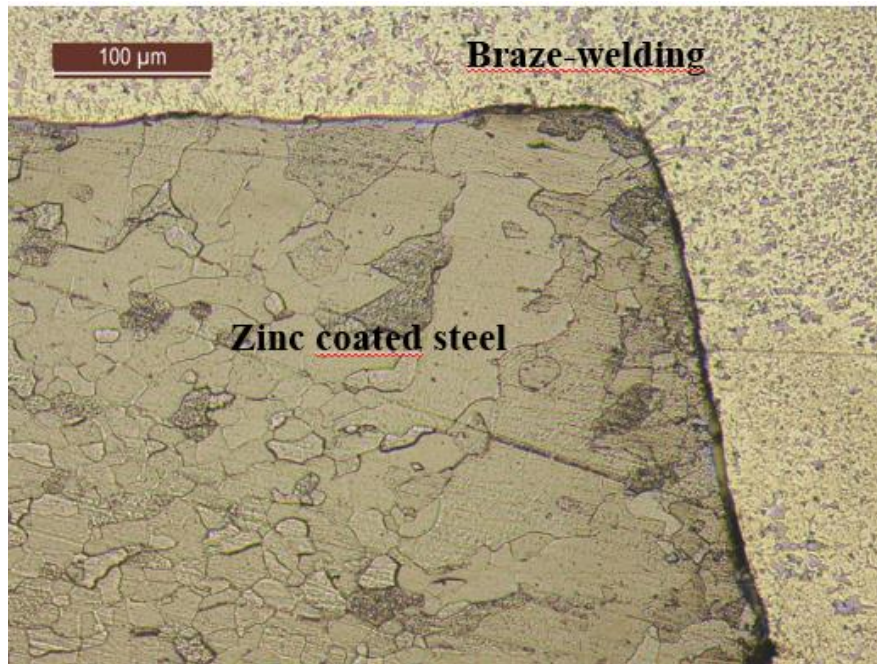
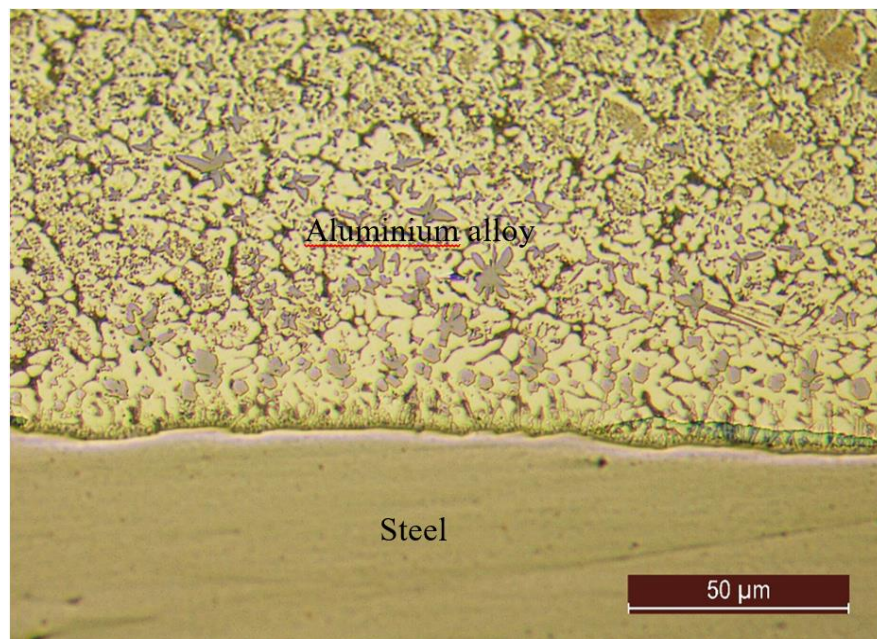


Fig.3.15 Macrographic image of a weld-brazed joint cross section

The beneficial effect of the zinc coating of the steel sheet on the wetting conditions is noticeable, ensuring a good connection between the weld and the surface of the galvanized sheet. The presence of the zinc layer (element with a melting temperature of 419 ° C) on the steel surface favors the dissolution of the surface alumina (Al_2O_3) and thus the melting of the aluminum alloy becomes possible without the use of a stripping flux.



(a)

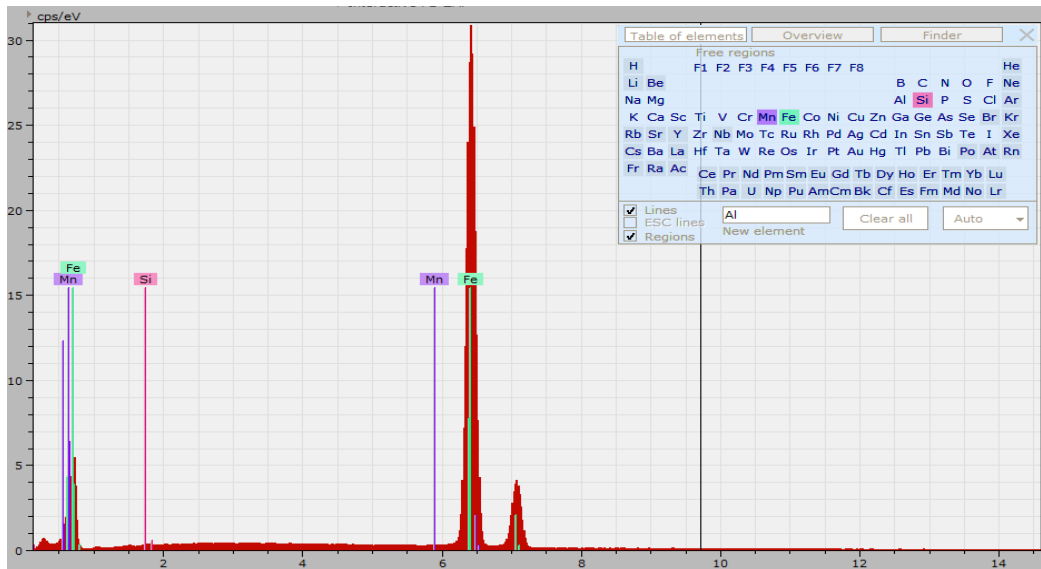


(a)

Fig.3.16 Micrographic image of a weld-brazed joint cross section: (a) the area of connection between the weld and the surface of the galvanized sheet; (b) Weld-zinc coated steel interface

3.3. EDX investigations

By melting a certain proportion of the base metal, Al alloy and mixing it with the filler material, a change in the chemical composition of the molten area occurs. Fig.3.17... 3.19 shows the images of energy dispersion of X-rays and the results of chemical analyzes in the areas of the south-brazed joint.

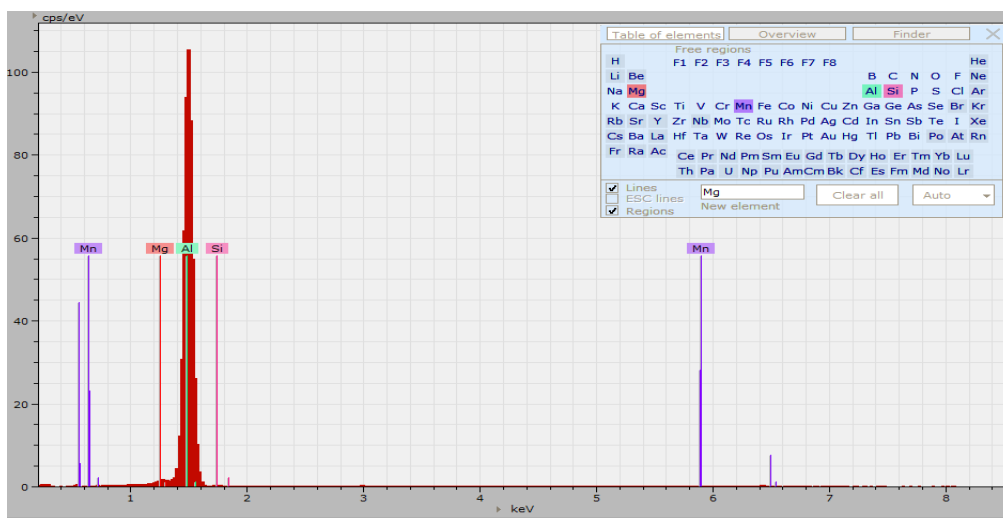


(a)

	Series	unn. C [wt.%]	nor. C [wt.%]	Atom C [at.%]	Error (1 Sigma) [wt.%]
Manganese	K series	1.66	1.56	1.59	0.07
Iron	K series	104.40	98.27	98.09	2.66
Silicon	K series	0.17	0.16	0.32	0.04
Total		106.24	100.00	100.00	

(b)

Fig. 3.17 EDX spectrum (a) and chemical composition of the steel component (b)

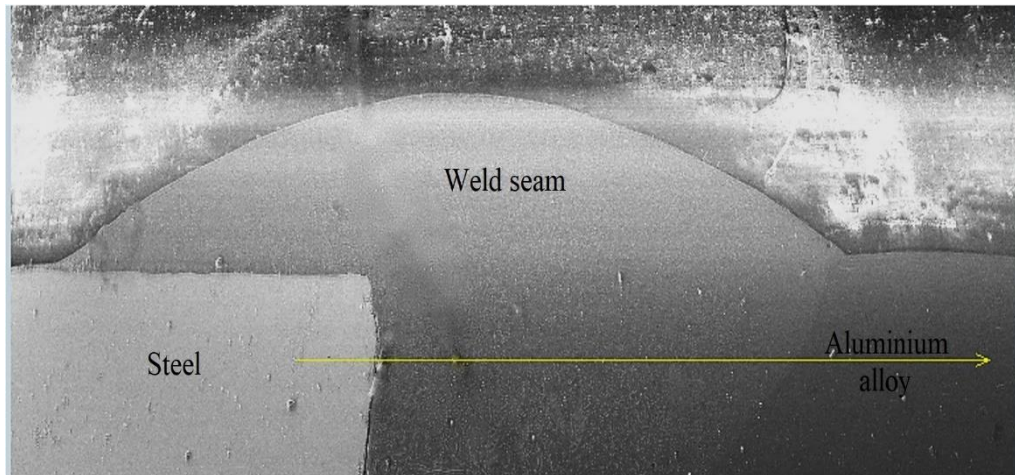


(a)

	Series	unn. C [wt.%]	nor. C [wt.%]	Atom C [at.%]	Error (1 Sigma) [wt.%]
Silicon	K series	1.29	1.21	1.16	0.09
Aluminium	K series	103.10	96.89	97.04	5.19
Manganese	K series	0.56	0.52	0.26	0.04
Magnesium	K series	1.47	1.38	1.54	0.11
	Total	106.42	100.00	100.00	

(b)

Fig. 3.18 EDX spectrum (a) and chemical composition of the Al alloy component (b)



(a)



(b)

Fig. 3.19 Macrograph image (a) and linear variation of the main chemical elements at the interface between the braze-weld bead and galvanized steel

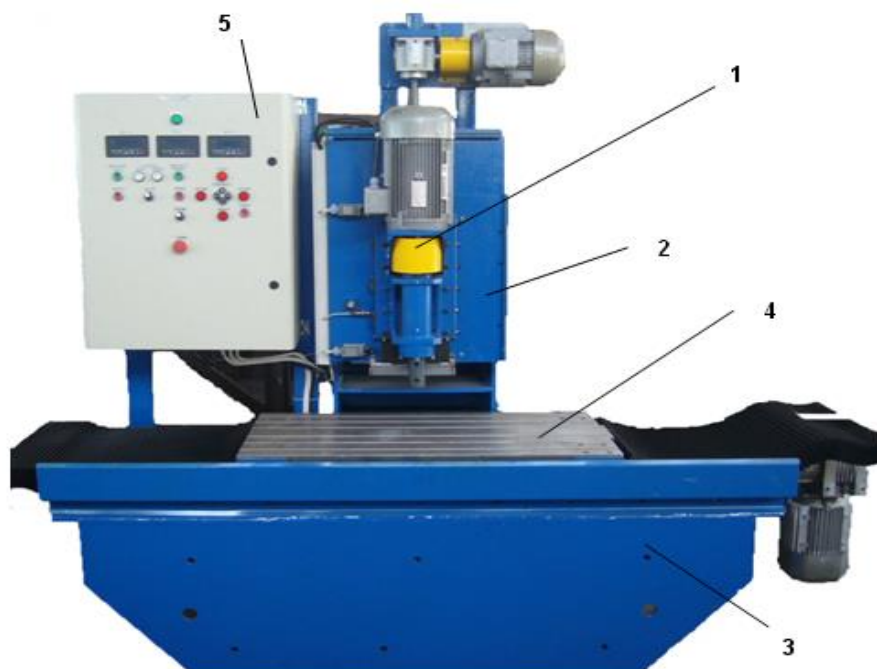
3.4. Conclusions

The difficulties encountered in joining by welding dissimilar materials, such as aluminum alloys and steels, are due to the differences in their physical properties (melting temperatures, thermal conductivity, coefficients of expansion). Obtaining the brazed-welded joint takes place by melting the basic material from the aluminum alloy, 6082 T6 and mixing it with the filler material, AlSi12, and at the moment of solidification the welded seam between the two alloys arises; at the same time, following the capillary wetting of the steel component by the liquid, a brazed connection is formed, so that in the end a sudo-brazing cord is obtained.

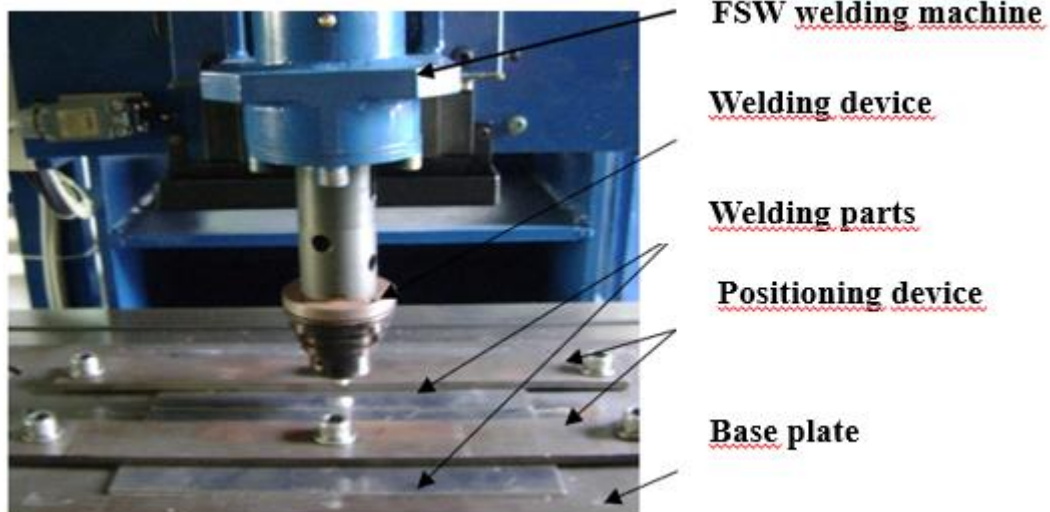
To avoid melting of the steel component, the laser beam must be positioned on the aluminum alloy component at a distance of 0.2 mm from the axis of the welding joint. High speed cooling, limits the thickness of the layer of fragile intermetallic compounds to 10 - 12 μm which can induce cracks in the weld and a reduction in mechanical strength characteristics.

Cap.4 Experimental research on the friction stir welding process

4.6. Experimental program



(a)



(b)

Fig. 4.8 FSW welding machine : a – overview; b - joint system detail

Tab. 4.1 Welding parameters

Nr. crt.	Materiale couple	Material thickness, s [mm]		Welding speed v [mm/min]	Tool rotation speed n [rot/min]	Welding tool material
		Up	Down			
1	Al 6082 – AISI 304	5	5	26 mm/min.	400	WC

4.7.1. Metallographic examinations

The optical micrographs are shown in fig. 4.10... 4.13. The base metal of Al alloy contains grains elongated in the direction of deformation and fine particles of intermetallic compounds (fig.4.10).

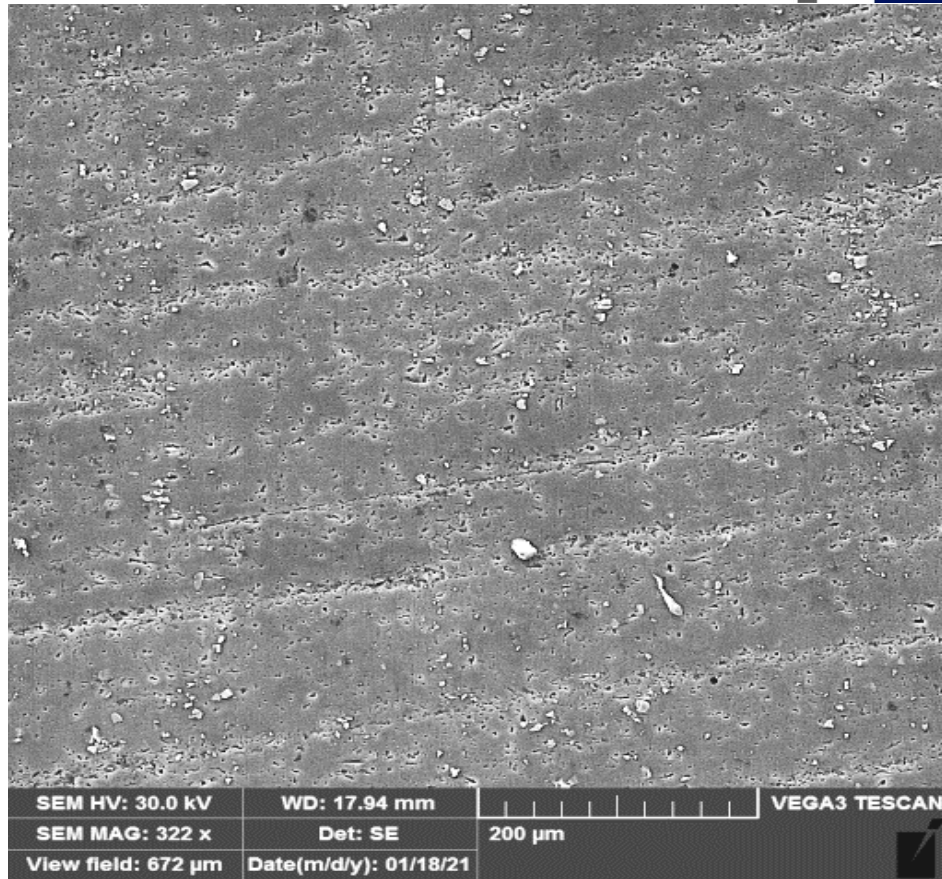
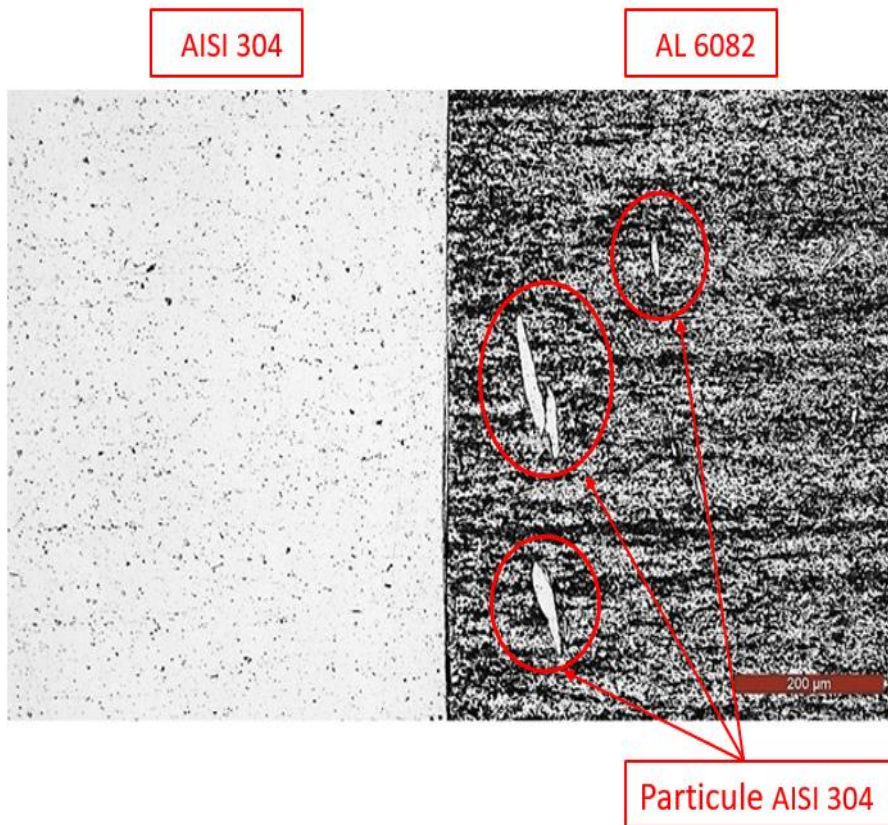
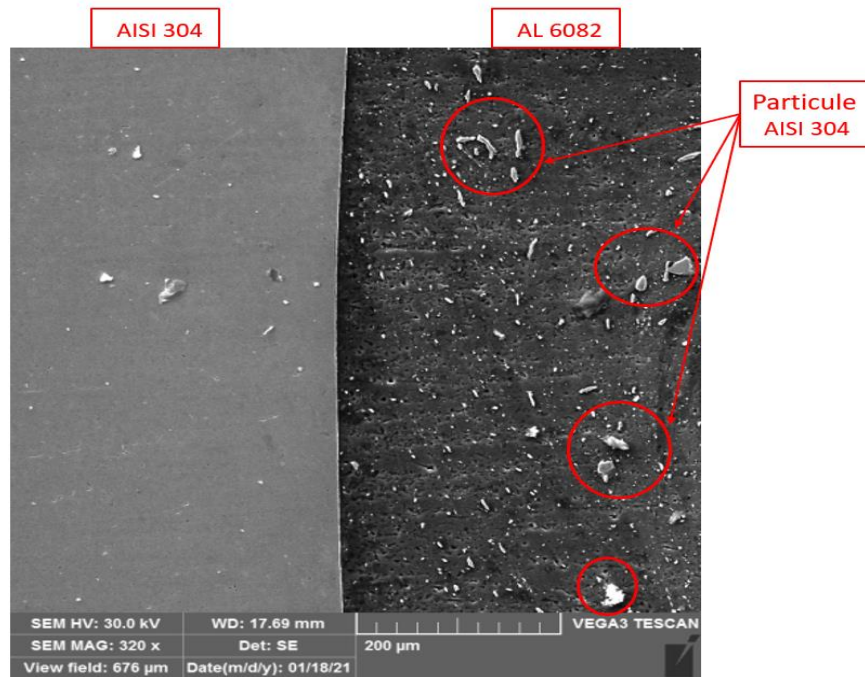


Fig.4.10 SEM micrograph of aluminum alloy



(a)



(b)

Fig.4.11 Structural image of a section by welded joint: a - optical microscopy; b- SEM microscopy

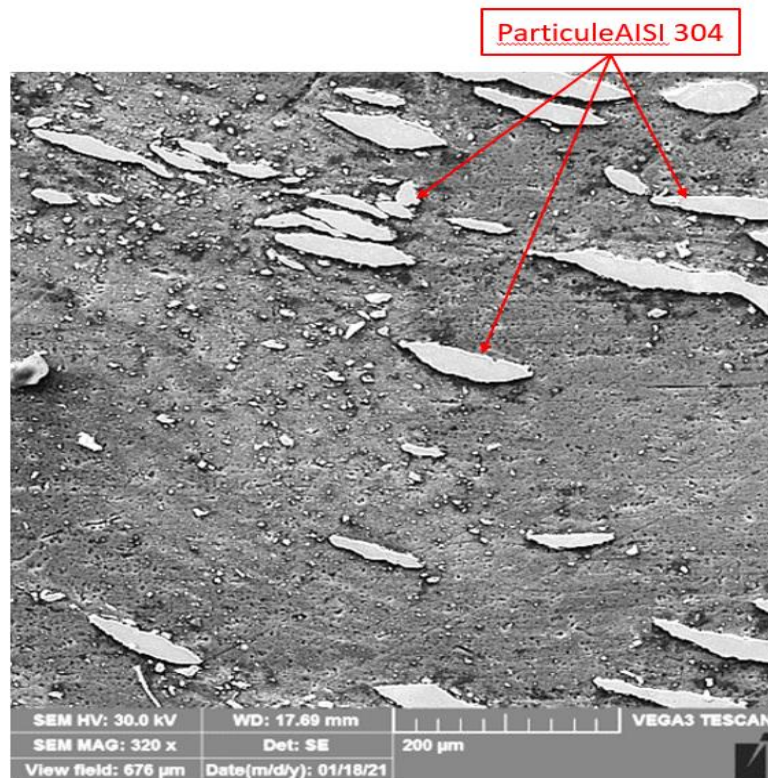


Fig.12 Weld nugget SEM microstructure

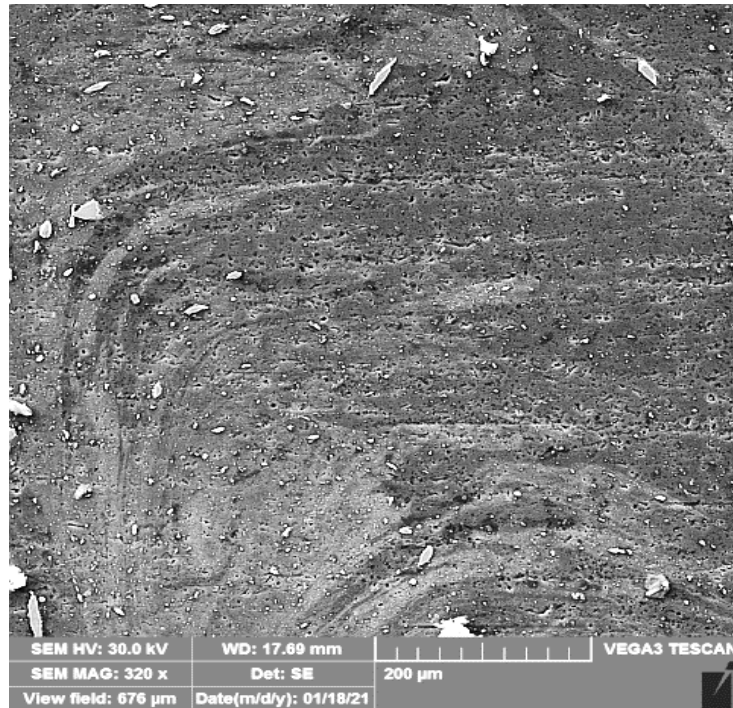


Fig.4.13 TMAZ SEM image of Al alloy

Between ZITM and the base metal of unaffected aluminum alloy on the withdrawal side appears a thermally influenced area, ZIT, characterized by lower and lower temperatures in which slight over-aging phenomena occur.

The stainless steel base metal has a microstructure consisting of austenite grains with a small proportion of ferrite δ and Cr₂₃C₆ complex carbides (fig.4.14). The ZIT microstructure of the stainless steel in the advance part is almost similar to that of the base metal, not thermomechanically affected (fig.4.15). In the thermomechanically influenced area of stainless steel, the presence of a certain proportion of σ phase is observed (fig.4.16, 4.17).



Fig. 4.14 Microstructure of base metal stainless steel

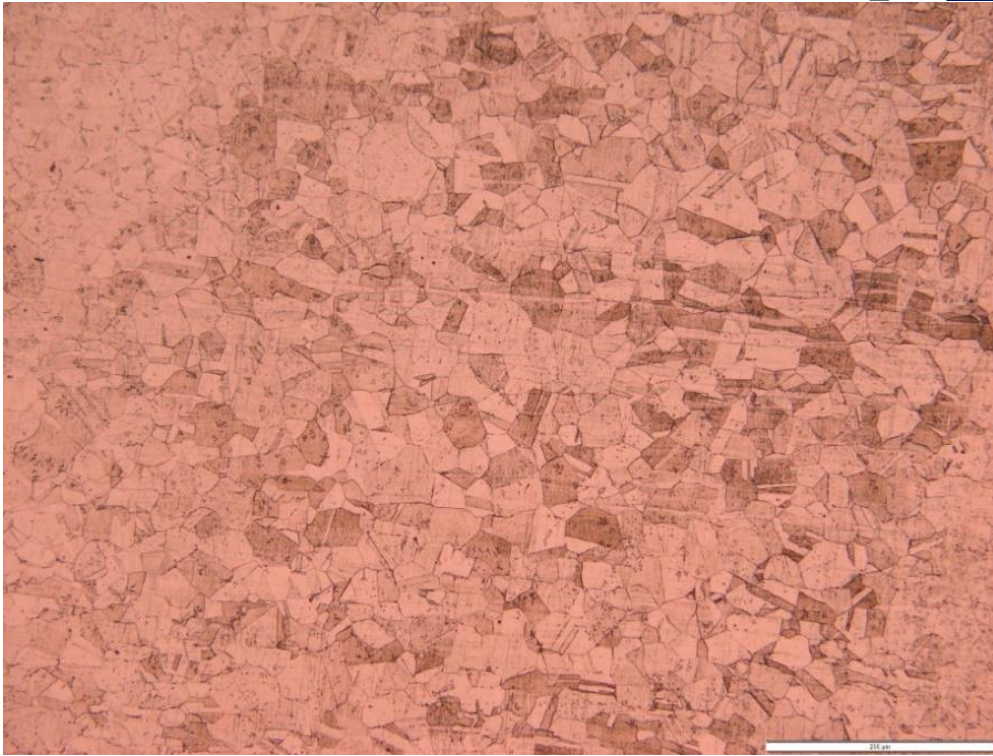
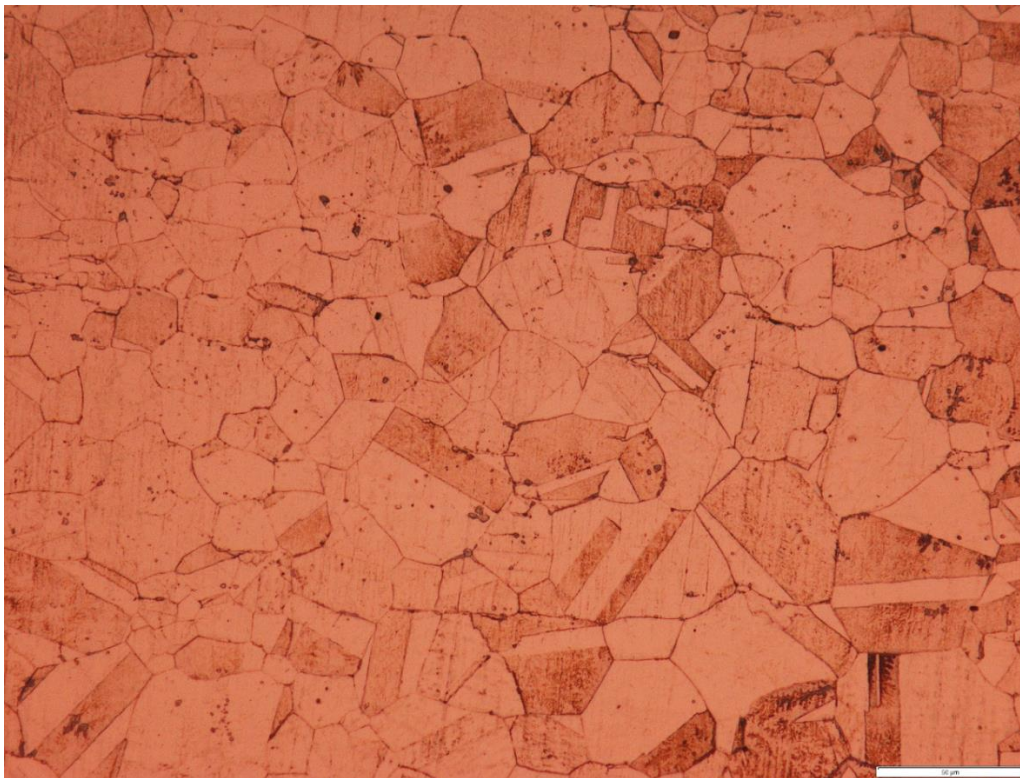


Fig. 4.15 Stainless steel HAZ



(a)

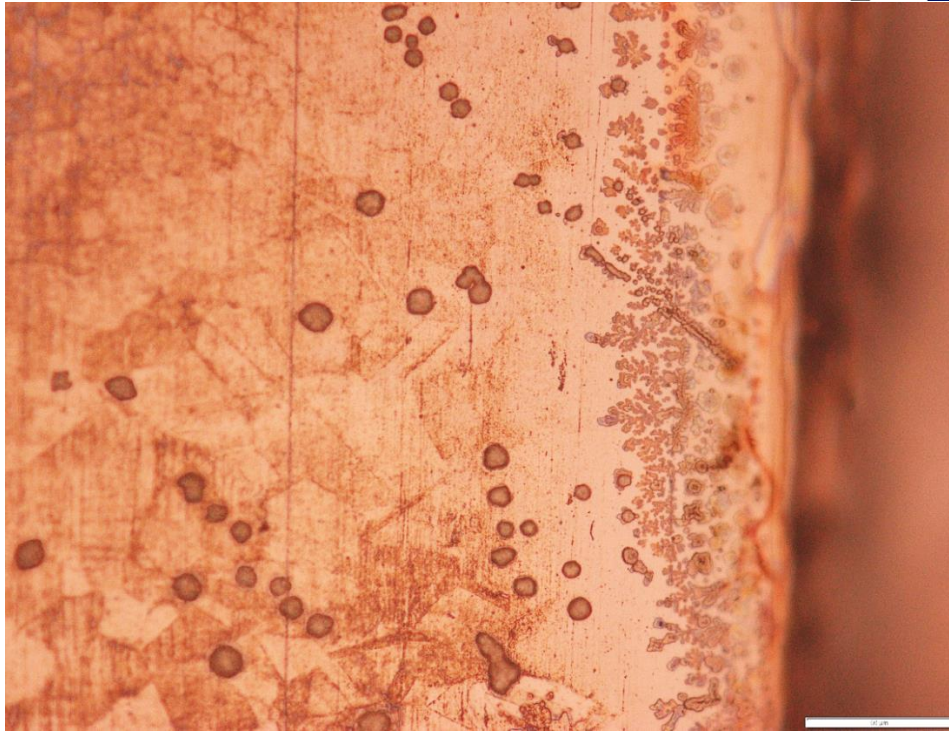


(b)

Fig.4.16 Microstructure of stainless steel in TMAZ: a –x 500; b – x 1000



(a)



(b)

Fig. 4.17 Stainless steel microstructure in the area of the interface with the weld nugget: a – x200; b – x1000

4.8. Conclusions

The FSW technique is suitable for joining deformable aluminum alloys with low carbon content austenitic stainless steels.

The microstructure of the FSW joints between the two dissimilar materials contains several characteristic areas determined by the developed temperature level, the degree of deformation reached and the time elapsed between the peak temperature and the thermal recrystallization threshold..

Cap.5 Final conclusions and original contributions. Future research directions

The main conclusions and original contributions of the paper can be summarized as follows:

1. Establishment by experiment of the optimal parameters of the MIG welding process in pulsed current, which should ensure the formation of joints without continuity defects such as cracks, shrinkage recesses, slag inclusions and porosity.

2. Highlighting the particularities of the primary and secondary crystallization process of the molten metal bath.
3. Structural changes in welding and ZIT (large grains, eutectic mechanical mixtures easily fusible the phenomenon of aging) is manifested by a reduction in the mechanical characteristics of welded joints.
4. Micrographic investigations in conjunction with EDX and X-ray diffraction analyzes scientifically substantiate the beneficial effect of post-weld heat treatment on microstructure restoration and improvement of the mechanical properties of the welded joint.
5. The joining by welding of aluminum alloys with galvanized steels encounters a series of difficulties due to the differences in their physical properties (melting temperatures, thermal conductivity, coefficients of expansion). The application of laser brazing, characterized by a high linear energy and high speed cooling, allows to avoid these difficulties by allowing a combination of the two materials without passing the steel into the liquid state.
6. Optimal parameters of the welding process of the aluminum alloy Al 6082 - T6 with a galvanized C-Mn steel using as additive material an aluminum alloy wire, AlSi12, ensures a good continuity of the weld bead, a good wetting of the galvanized steel sheet and a penetration of the weld over the entire section of the galvanized sheet without leakage of material at the root.
7. Examination of the cross-sections by laser and brazed laser joints under a scanning optical and electron microscope revealed an appropriate fusion between the filler material and the aluminum alloy base material, obtaining a sufficient thickness of the weld brazing cord, a limitation to 10 - 12 μm of the layer thickness of fragile intermetallic compounds, FeAl₃, and the lack of continuity defects that can constitute breaking primers.
8. Microscopic observations on the reaction area between the Fe and Al atoms showed the beneficial effect of the zinc coating of the steel sheet on the wetting conditions, ensuring a good connection between the weld and the surface of the galvanized sheet. The presence of the zinc layer favors the melting of the aluminum alloy and acts as a chemical barrier delaying the reaction between aluminum and steel and limiting the heat flow transmitted to the steel and thus the temperature of the area on which liquid aluminum is deposited. The use as an additive of AlSi12 alloy with a chemical composition close to the eutectic one favors the melting of the eutectic and implicitly a reduction of the energy intake.
9. X-ray energy dispersion spectra, together with the results of quantitative chemical analyzes in microvolumes of material, have shown that on the cross section of welded joints there are variations in restricted concentrations in alloying elements determined mainly by the peculiarities of the welding process. laser beam brazing.
10. The rotary active element friction welding technique, FSW, can be successfully applied for joining deformable aluminum alloys with austenitic stainless steels.
11. The microstructure of the welded joint is divided into several characteristic subzones, the hardness of the welding core has variable values due to the presence of fine or coarse particles of stainless steel dispersed in it. The hardness value in the retracting part

decreases suddenly towards the welding core, from the thermo-mechanically affected area of the stainless steel to the advance part of the weld. In contrast, in the advance part (Al 6082-T6 alloy part), the hardness value decreases slightly in the thermomechanically influenced area.

Bibliography

- [2] A. Mathieua, S. Pontevicci', J. Vialab, E. Cicala, S. Matti, D. Grevey, Laser brazing of a steel/aluminum assembly with hot filler wire (88% Al, 12% Si), *Materials Science and Engineering A* 435-436 (2006) 19-28.
- [11] F. Haidara, M.-C. Record, B. Duployer, D. Mangelinck, Phase formation in Al-Fe thinfilmsystems, *Intermetallics* 23 (2012) 143-147.
- [30] I. Mitelea, E. Lugscheider, W. Tillmann: *Stiinta materialelor in constructia de masini*. Editura Sudura, 1999
- [32] ISO 209-1:2007, *Aluminium and Aluminium Alloys-Chemical Composition*, January 01, 2007, International Organization for standardization.
- [36] J. L. Song, S. B. Lin, C. L. Yang, G. C. Ma, H. Liu, Spreading behavior and microstructure characteristics of dissimilar metals TIG welding-brazing of aluminum alloy to stainless steel, *Materials Science and Engineering A* 509 (2009) 31-40.
- [37] Kluken, A. O., Bjoernekleit, B.: A study of mechanical properties for aluminium GMA weldments, *Welding Journal*, 76(2), (1997), pp. 39 – 44.
- [41] L. Agudo, D. Eyidi, C. H. Schmaranzer, E. Arenholz, N. Jank, J. Bruckner, A. R. Pyzalla, Intermetallic FeAl₃-phases in a steel/Al-alloy fusion weld, *Journal of Materials Science* 42(2007) 4205-4214.
- [47] M. Dehghani, A. Amadeh, S.A.A. Akbari Mousavi, Investigations on the effects of friction stir welding parameters on intermetallic and defect formation in joining aluminum alloy to mild steel, *Materials and Design* 49 (2013) 433-441.
- [48] M. J. Torkamany, S. Tahamtan, J. Sabbaghzadeh, Dissimilar welding of carbon steel to 5754 aluminum alloy by Nd: YAG pulsed laser, *Materials and Design* 31 (2010) 458-465.
- [67] S.B. Lin, J.L. Song, C.L. Yang, C.L. Fan, D.W. Zhang, Brazability of dissimilar metals tungsten inert gas butt welding-brazing between aluminum alloy and stainless steel with Al-Cu filler metal, *Materials and Design* 31 (2010) 2637-2642.
- [78] V. T. Witusiewicz, A. A. Bondar, U. Hecht, and T. Y. Velikanova, Phase equilibria in binary and ternary systems with chemical and magnetic ordering, *Journal of Phase Equilibria and Diffusion* (2011) 32:329-349.
- [83] *Warmebehandlung von Aluminiumlegierungen* ISBN 978-3-937171-19-7 | GDA-07-09 | 1.000 | 09-2007 – pag.03-21 – (Bild 1..7; Tabelle2,3a).